Hindawi
Advances in Materials Science and Engineering
Volume 2022, Article ID 7263333, 15 pages
https://doi.org/10.1155/2022/7263333

Research Article

Consolidated Drained Triaxial Test on Treated Coastal Soil and Finite Element Analysis Using PLAXIS 2D

Zahraalsadat Elias Lankaran, Nik Norsyahariati Nik Daud, Vahid Rostami, and Zainuddin Md. Yusoff

Civil Engineering Department, Engineering Faculty, Universiti Putra Malaysia, Seri Kembangan, Malaysia

Correspondence should be addressed to Zahraalsadat Elias Lankaran; nina_5950@yahoo.com

Received 13 April 2022; Revised 9 September 2022; Accepted 11 October 2022; Published 24 November 2022

Academic Editor: Qian Chen

Coastal areas are susceptible to erosion and accretion; therefore, coastal soil mechanical properties and ability to withstand loads are important factors to consider. Coastal erosion is inevitable as the sand and silt particles move inexorably from place to place. This study investigates the primary consolidation behaviour of treated coastal soil by comparing the empirical data obtained from triaxial tests based on analytical calculations and FEM software, PLAXIS 2D. The aim is to propose an optimum mixture to improve coastal soil's geotechnical properties, especially in shear strength and stiffness. Two different material models, including lime/RHA and cement/RHA, were utilized to compare the performance of advanced constitutive treated soil samples against the Mohr–Coulomb material model. 8% lime and rice husk ash (portions of 1 : 2) were chosen to be replaced with cement, as an application of waste material can reduce the cost and environmental impact. All the triaxial tests were conducted at effective confining pressures of 50 kPa, 100 kPa, and 200 kPa. While using PLAXIS 2D, the asymmetrical condition for modelling the triaxial test and 15 nodded triangular elements, as well as the Mohr–Coulomb model for soil properties, are used to simulate the empirical data to verify this study's effectiveness. The modelling of 2-dimensional drain behaviour involves setting out the model geometry and boundary conditions. The results revealed that the deviatoric stress and volumetric changes of LRHA increased in a range of 4.5 to 5.2% and 72.18 to 141.79%, respectively, as compared to CRHA. The FE analysis results for peak deviator stress values reasonably agree with the experimental results. The variation was in the range of 1.22% to 4.10%. Eventually, the treated soil's peak and maximum shear strengths are reported to allow flexible use in future projects.

1. Introduction

Sea level rise and extreme events related to climate change are causing severe threats to coastal areas, affecting both natural and human systems worldwide [1, 2]. According to grain size analysis, the coastal sediment consists of medium- to fine-grained sand, silt, and clay. This soil with the features of high compressibility and low shear strength are categorized as problematic soils [3].

The work detailed within this technical study was concerned with the simulation of triaxial tests on soil treated with lime-rice husk ash (LRHA) and cement-rice husk ash (CRHA), with the aim of gaining insight into the mechanical behaviour of stabilized soils for geotechnical applications, ground engineering, and suggesting low-cost alternative mixtures to cement with environmentally friendly characteristics [4, 5]. The numerical approach enables the determination of material parameters that would have been difficult to measure in the experimental study. PLAXIS is an advanced geotechnical software developed to analyze the aspects of stability and deformation in geotechnical engineering problems and conduct finite element analysis to determine the soil behaviour. This numerical simulation method was used to determine the effects of the modelling parameters on soil strength predictions and to compare, correlate, and verify between the laboratory tests and the computer modelling [6, 7], and it consists of three steps: input, calculation, and output. Recently, little research has been carried out assessing the benefits, limitations, and challenges that follow when modelling in PLAXIS using the

soft soil material instead of modelling with the Mohr–Coulomb model for a geotechnical problem [8].

In fact, PLAXIS is a finite element code for soil and rock analyses, originally developed for analyzing deformation and stability in geotechnical engineering and soil modelling techniques that have been developed rapidly over the last 20 years [9]. The material model in PLAXIS simulation can be regarded as a qualitative representation of the behaviour of a sample, whereas the model parameters can be used to quantify the behaviour of the sample. Most previous research in Malaysia using PLAXIS software has been conducted in the form of in situ to determine solutions for minimizing deformation, demonstrating the effect of preloading in peat soils as well as estimating and improving the soil shear strength, which was part of this study [10]. Also, PLAXIS modelling was used in studies to simulate a safe height for embankments on soft soil [11, 12].

2. Experimental Program Work

A wide range of triaxial tests were performed on soil treated with lime and rice husk ash as well as samples treated with cement/RHA and validated with the finite element simulation. The treated soil samples with 8% lime and RHA in portions of 1 : 2 and 8% of cement/RHA in portions of 1 : 2 (LR8 and CR8), which mimicked the strength parameters entered in the numerical models, consisted of 8% lime mixed with 16% rice husk ash (LR8) and 8% cement mixed with 16% rice husk ash (ratio of 1 : 2) and water, were left to equilibrate for 24 hours. The treated samples were cured for 28 days, according to ASTM-D 1632. All the treated samples were prepared at their optimum moisture content. The treated soil was shaped in a cylindrical mold with a height of 10 cm and a diameter of 5 cm, as shown in Figure 1.

2.1. Consolidated Drained Triaxial Behavior of Treated Soil. One of this project's objectives is to carry out triaxial tests to understand the mechanical behaviour and analyze the treated soil. The triaxial test is one of the most precise geotechnical tests and accurate methods for determining soil strength and stress-strain properties. By performing this test, parameters such as strength and deviatoric stress, pore pressure, and volume changes, can be recorded [13]. According to ASTM-D7181, in a consolidated drained (CD) test, the sample is consolidated and slowly sheared under compression to allow pore pressure to build up as the shearing dissipates.

In the triaxial test method, soil samples are placed between two metal plates, and then, vertical pressure is applied to the parallel metal plates and lateral pressure is applied using water. Applying the compressive stress creates and expands shear stress inside the specimen. The triaxial test equipment reports the deformation and increases the load until the failure of the samples. In the final stages of the experiment, a decrease in height and a bulge on the sides occur. At this stage, by reducing the compressive stress of the plates and increasing the compressive stress of the surrounding fluid, a further increase in the height of the samples was recorded.

Three shear tests under different normal vertical loads of effective stress (50 kPa, 100 kPa, and 200 kPa), as indicated by LR8-50, LR8-100, and LR8-200, and CR8-50, CR8-100, and CR8-200, were carried out to obtain the soil strength parameters. The physical properties of pure soil is shown in table 1.

Table 2 shows the mix design of aggregates, pozolan and water mixed in treated samples. The axial load was applied at a constant rate (0.001 mm/min). The load was applied to the soil sample through the loading ram, and it was recorded through the load cell. The deviator stress was obtained as the applied axial load was divided by the effective area of the specimens.The LRHA-treated samples demonstrate a single-incline failure plane under the triaxial stress. Treated LRHA soil under consolidated drain triaxial compression under the confining pressure of 200 kPa displays very similar deformation and inclination angles, while the CRHA samples show a sharp inclination of 90° under 200 kPa confining pressure (Figure 2).

3. Analysis of Obtained Results from the Triaxial Drained Consolidation Test

The analysis of obtained results from the triaxial drained consolidation test is as follows.

3.1. Mohr–Coulomb Strength Parameters. Shear stress parameters are found by drawing Mohr–Coulomb circles. Figures 3 and 4 graphically present the shear strength envelope of the saturated specimens that were sheared using the CD single-stage method with effective confining stresses of 50, 100, and 200 kPa. It was observed that all the samples failed at various axial strains.

The following formula and shear strength (τ) are accepted just for shear stress on the failure plane:

$$\tau_f = c + \sigma' (\tan \varphi), \tag{1}$$

where c is cohesion (kPa), ϕ is the angle of internal friction (degree), and σ' is effective stress (kPa). Mohr–Coulomb failure criteria have been used to define the soil stress concept. Stress conditions at failure in a soil mass are given in Figures 3 and 4.

If the failure plane makes an angle θ with the major principal plane, the normal stress and the shear stress on the plane are given as follows:

$$\sigma = \frac{\sigma 1 + \sigma 3}{2} + \frac{\sigma 1 - \sigma 3}{2} \cos \quad \cos 2\theta, \tag{2}$$

$$\tau f = \frac{\sigma 1 - \sigma 3}{2} \sin\ 2\theta. \tag{3}$$

The behaviour of the LRHA-treated soil was similar to the axial strength-lime content curve, where at the optimum lime content, the cohesion became stable; while beyond this optimum content, the value of c' was relatively constant. The

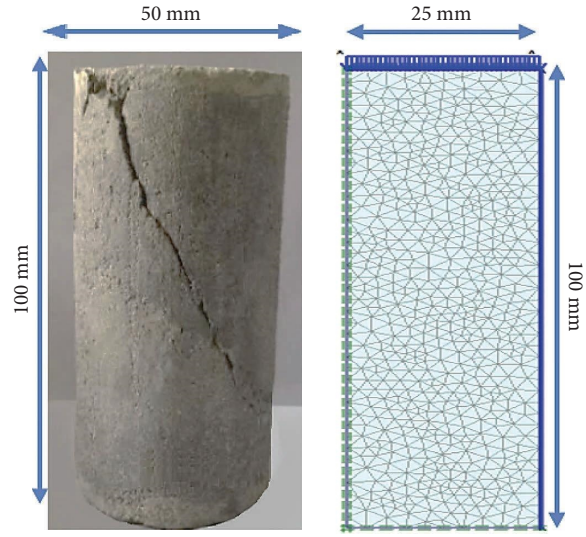

Figure 1: (a) The exact model (50 mm by 100 mm) and (b) typical axisymmetric geometry model (25 mm by 100 mm).

Table 1: Physical properties of West Coast soil.

Properties	Unit	Value
Moisture content	%	16.3
Specific gravity	—	2.63
Grain size analysis		
Sand	%	65–70
Silt and clay	%	30–35
USCS classification	—	SC-SM-CL
Consistency limit		
Liquid limit	%	47.5
Plastic limit	%	28
Plasticity index	%	19.5
Compaction study		
MDD	Mg/m^3	1.48
OMC	%	16.2

Table 2: Mix design of soil stabilizer and pozzolan values used in the experimental tests.

Specimen	*W*/*B*	Cement (%)	RHA (%)	Lime (%)	Cement (gr/cm^3)	RHA (gr/cm^3)	Lime (gr/cm^3)	Soil (gr/cm^3)
LR8	0.2	0	16	8	0	76.8	38.4	480
CR8	0.2	8	16	0	40.96	81.9	0	512

shear strength of the samples treated with 8% LRHA and cured for 28 days increased from 0.0138 MN/m^2 to 0.319 MN/m^2 and increased from 0.145 MN/m^2 in the CRHA-treated soil to 0.336 MN/m^2 after 28 days of curing.

An increase in curing duration from 7 to 28 days causes a remarkable increase in the shear strength. This could have been due to the formation of larger quantities of cementing materials and more cemented contact points in the mixture. A similar result has been reported by other researchers [14, 15].

3.2. Deviatoric Stress. Figures 5 and 6 demonstrate the stress-strain curves at effective stresses of 50, 100, and 200 kPa in the fully saturated condition. The curves indicate the typical three-step pattern in each deviatoric stress-strain curve. Figure 5 shows the axial strain (ε) versus deviatoric stress ($\Delta\sigma$) for samples treated with 8% LRHA and cured for 28 days.

The confining pressure and the deviator stress are applied to the failure. The maximum deviatoric stress appeared to increase significantly from the samples mixed with lime to the samples treated with LRHA as the effective stress increased from 50 to 200 kPa.

For the series of tests using the single-stage method, the specimen was compressed up to failure until the sample's strength was reached. The value of the axial strain in the stress-strain curve indicated that the axial deformation in the specimen was due to the related

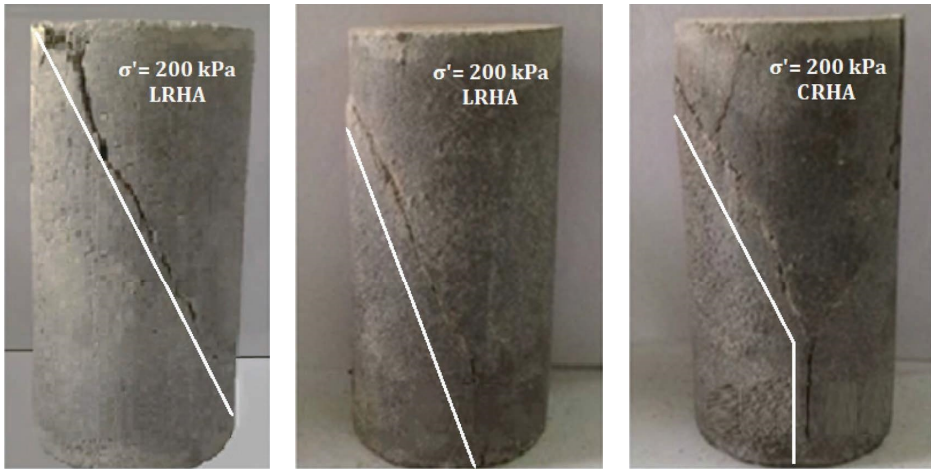

Figure 2: Comparison between CRHA and LRHA failure modes. (a) CRHA and (b and c) LRHA.

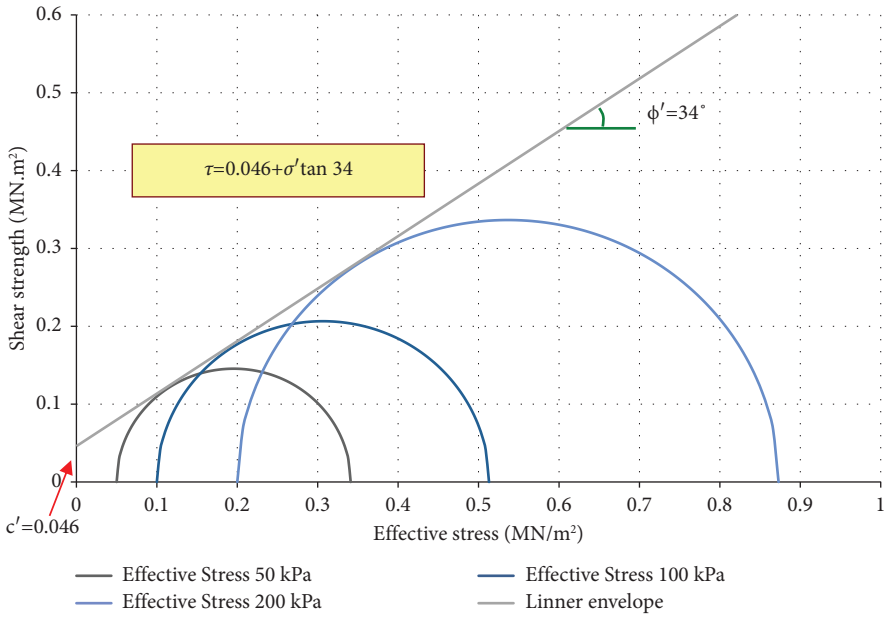

Figure 3: Shear strength variation against the effective stress-saturated condition LR8 (lime RHA 1 : 2, 8% lime content, and 28 days of curing).

deviatoric stress. For example, for a strain of 3.4% at an effective stress of 200 kPa in a saturated condition, the deviatoric stress was 600 kPa. In this condition, the specimen would settle at 10% of its initial height.

There was a sharp increase in the deviatoric stress over a small range of the axial strain at the beginning of the shearing stage. This was followed by a reasonably wide range of variations in the constant rate of the deviatoric stress in relation to the axial strain, where the samples failed when the maximum deviatoric stress was reached. Effects of lime stabilization on soft soil, with a very similar pattern, were also well confirmed by Song et al. [16] and Wang and Leung [17]. Wang conducted an undrained triaxial test on Ottawa sand treated with cement. The deviatoric stress versus strain graph shows a sudden and strong increase in deviator stress values. After reaching the peak, the curves start to decline. The rate of deviatoric stress falls after the peak due to sample shearing and the failure stage. At this point, a steady reduction in the deviatoric stress values with axial strain occurs, followed by a residual state of the deviatoric stress, which eventually becomes steady on a horizontal line. The similar pattern was reported by Wang [17]. Strain and deviator stress values are close to what has been recorded in this research. The difference in the deviatoric stress of the LRHA-treated soil at an increase of 3.4% in strain from 50 to 200 kPa was 445 kPa. After the greater deformations, the average coordination number remains practically constant until the end of the tests.

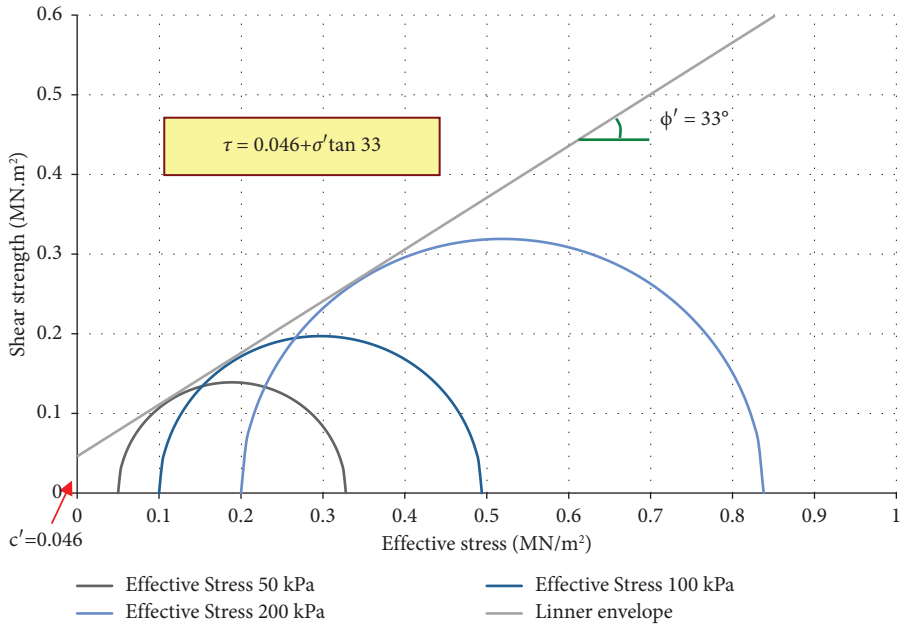

Figure 4: Variation of shear strength against the effective stress-saturated condition CR8 (cement RHA 1 : 2, 8% cement content, and 28 days curing).

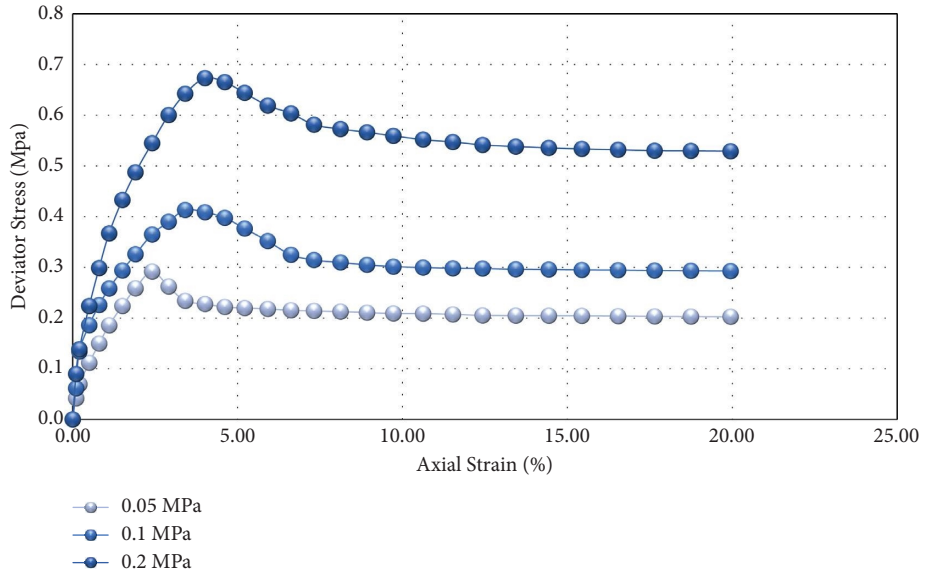

Figure 5: Deviator stress-strain curves for sample LR8 (8% LRHA treated soil 1 : 2) after 28 days.

3.3. Volumetric Changes. Figures 7 and 8 show the volumetric changes in samples treated with CRHA and LRHA (1 : 2) for 28 days.

The treated samples demonstrated a steady reduction in volume based on each effective confining pressure. In fact, the volume of the specimens decreased when the effective stress and root time were increased. The rate of reduction in the volume tended to vanish when the deviatoric stress approached the failure state. During the shearing, the soil particles tended to be rearranged and to expel the pore water.

The tests' evaluation showed that the variation in shear strength of differently treated samples was related to the effective normal stress in a saturated condition, where it was linear at a high-stress level at a minimum friction angle of $\phi = 33^{\circ}$.

The triaxial test results and the numerical simulation's geometry input are illustrated in Tables 3 and 4.

The specimens tested in the drained triaxial cell at particular initial conditions reach a limit at large deformation, at which the strength provided by the individual particles remains constant.

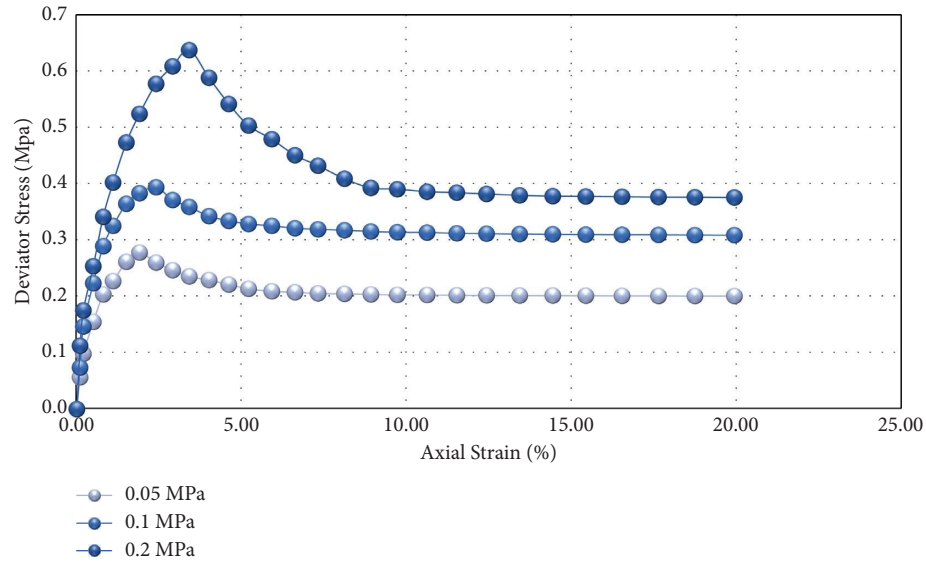

Figure 6: Deviator stress-strain curves for sample CR8 (8% CRHA treated soil 1 : 2) after 28 days.

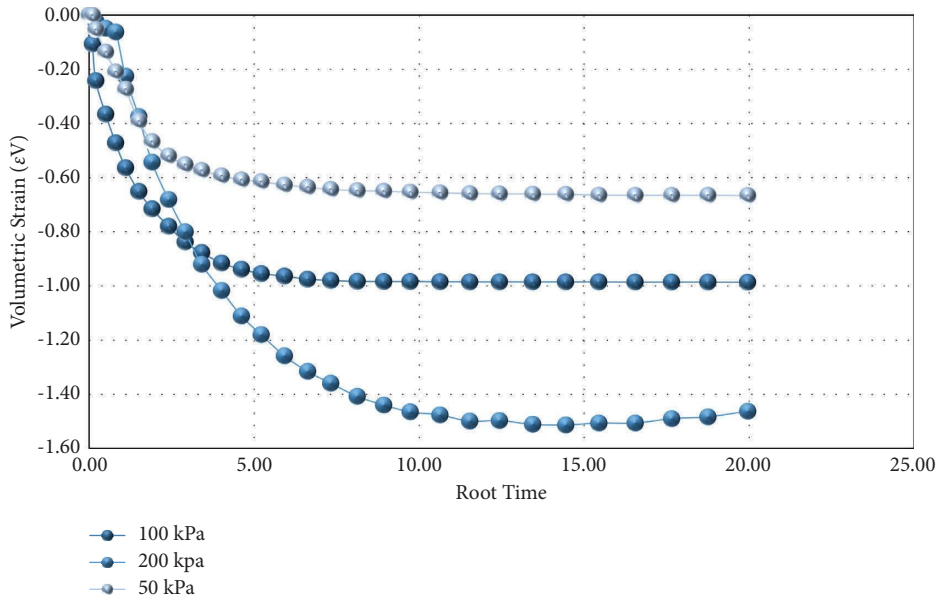

Figure 7: Volumetric changes in three effective confining pressures: CRHA-treated soil.

4. Finite Element Modelling

In this section, expert finite element mesh settings were used. As shown in Figure 1(b), the triaxial tests are modelled using simplified axisymmetric geometry. Three series of consolidated, drained triaxial tests on treated soil were modelled Figure 9. At this stage, an axisymmetric model with 15 nodes was applied to simulate a cylindrical specimen measuring 100 mm in height and 50 mm in diameter. Line loads were assigned to the right and top boundaries. The lateral stresses, σ_2 and σ_3, were represented by the distributed loads on the right and front, respectively. The axial stress, σ_1, was represented by a distributed load on the top of the model.

The mesh creation took full account of the positions of the points and lines in the geometrical model so that the exact positions of the loads were considered in the finite element mesh [18].

4.1. Numerical Analysis of Treated Soil Samples during the Triaxial Test. The 15-node elements were employed in the simulation of soil elements. Therefore, each geogrid element was defined by fifteen node line elements, which automatically act as membranes, and hoop stress can be determined on the encasement. 15-node element offers more guess points compared to 6-node, which leads to a more precise determination of displacements and stresses. The model's

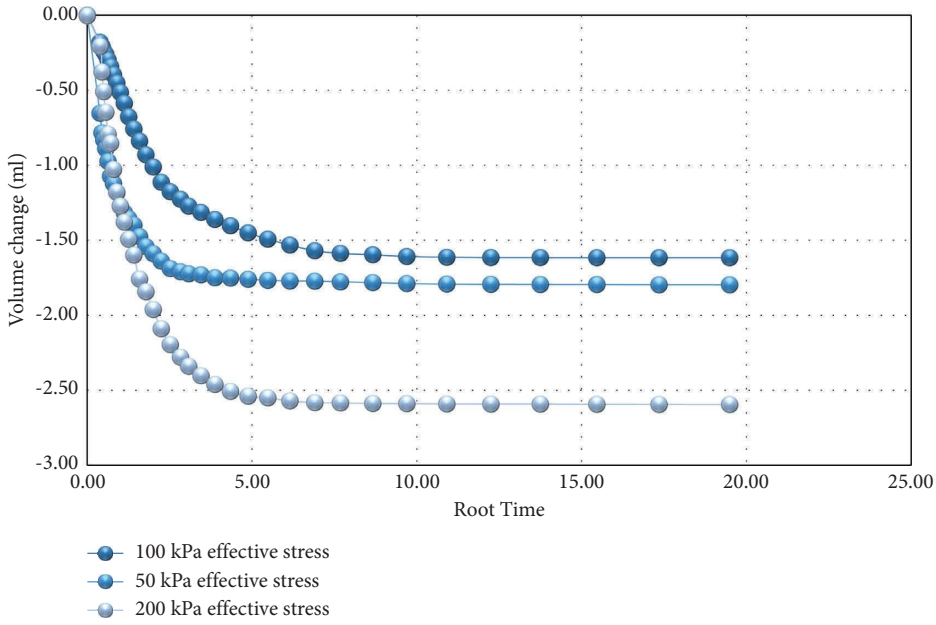

Figure 8: Volumetric changes in three effective confining pressures: LRHA-treated soil.

Table 3: LRHA-treated soil (LR8) mechanical parameters.

Treated samples with 8% LRHA 1 : 2, 28 days						
Test ID	σ_3 (MN/m^2)	q (MN/m^2)	σ_1 (MN/m^2)	ϕ (degree)	c' (MN/m^2)	τ (MN/m^2)
LR8-50	0.05	0.291	0.341	34	0.046	0.07972543
LR8-100	0.1	0.431	0.531	34	0.046	0.11345085
LR8-200	0.2	0.673	0.873	34	0.046	0.1809017

Table 4: CRHA-treated soil mechanical parameters.

Treated samples with 8% CRHA 1 : 2, 28 days						
Test ID	σ_3 (MN/m^2)	q (MN/m^2)	σ_1 (MN/m^2)	ф (degree)	c' (MN/m^2)	τ (MN/m^2)
CR8-50	0.05	0.278	0.328	33	0.046	0.07847038
CR8-100	0.1	0.394	0.494	33	0.046	0.110940759
CR8-200	0.2	0.638	0.838	33	0.046	0.175881519

dimension also is in accordance with the 15-node triangles. 15-node element correlates well, so the deformation in the soil does not intersect the model's boundaries. Figure 10 shows the variation of the total displacements of the treated samples under three-dimensional loading. The length of the samples shortened, while the width in the lateral axis increased. After performing the tests, LRHA 8%-50, LRHA 8%-100, and LRHA 8%-200, the total displacements exceeded 4.39 mm, 4.35 mm, and 5.31 mm, respectively. On the other hand, the maximum total displacements of cement-treated samples were quite varied. The total deformed mesh for samples CRHA 8%-50, CRHA 8%-100, and CRHA 8%-200 were 2.93 mm, 8.75 mm, and 7.97 mm, respectively.

4.2. Stress-Strain Behaviour. Figures 11–13 demonstrate the numerical and experimental results, including values of displacements, stresses, boundary conditions, and material clusters, as well as the strains obtained from the triaxial test and PLAXIS modelling. The numerical simulation studies of LRHA and cement-RHA mixture samples with the ratio of 1 to 2, under three confining pressures (50, 100, and 200 kPa), were conducted and compared to laboratory samples. As shown in Figure 11, the stress-strain curves in all numerical modelling experiments are essentially identical to those obtained in laboratory tests. During the initial elastic stage, the numerical simulation results were slightly lower than the laboratory results, and as the confining stresses increased, the difference becomes greater in the middle part of the curve. At the failure stage, calculated deviator stresses represented the samples' strength in a bit higher value, with differences of 3%, 4%, and 2% for LRHA 8%-50, LRHA 8%-100, and LRHA 8%-200, respectively. In confining stresses of 50 kPa and 100 kPa, the calculated curves hit the peaks faster, while the specimens have smaller axial strains. It indicates that the numerical modelling displays the specimens with different stiffness that can be related to the modelling behaviour based on Mohr–Coulomb, which does not consider the stiffness based on the variation of pressure [10].

It can be seen from Figure 12 that the stress-strain curves of CRHA tests in numerical simulation studies were below the laboratory test result in all stages except the

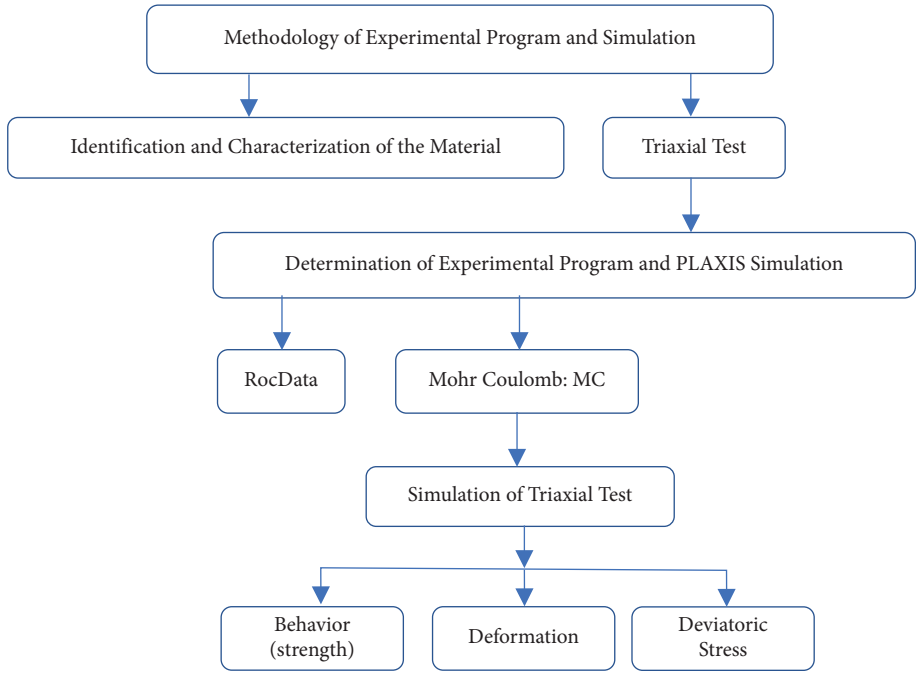

Figure 9: Methodology chart of the experimental and the numerical modelling.

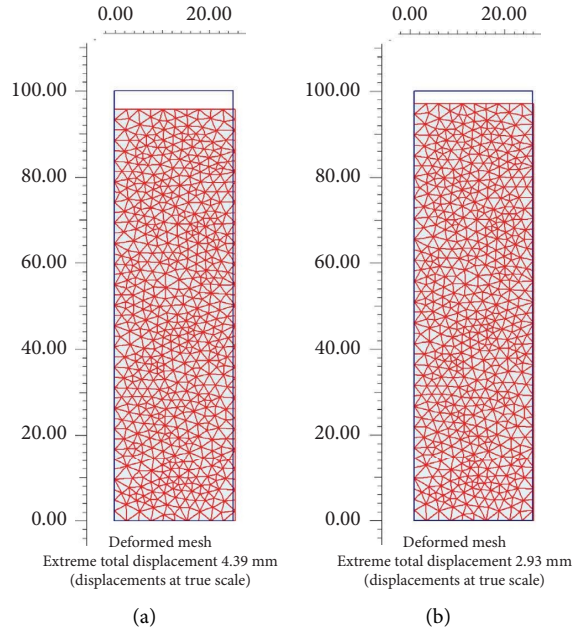

Figure 10: Deformed mesh (a) after the LR8_50 test and (b) after the CR8_50 test.

failure stages. In the failure stages, numerical modelling shows the calculated deviator stresses are very close to the measured data, with differences of 4%, 5%, and 2% for CR8-50, CR8-100, and CR8-200, respectively. Unlike the calculated deviator stresses for LR8-50 and LR8-100, in all CR8-50, CR8-100, and CR8-200 tests (Figure 12), the calculated curves hit the peaks later, while the specimens have bigger axial strains.

Changes to the geometry configuration cause a significant out-of-balance force. The finite element mesh is under a series of forces using the load advancement ultimate level procedure.

In Figure 13, the graphs compare the deviator stress versus axial strain in LRHA and CRHA samples under three different confining stresses. It can be seen that the increasing rates of axial strain for both LRHA and CRHA mixtures behave similarly, especially at confining stresses

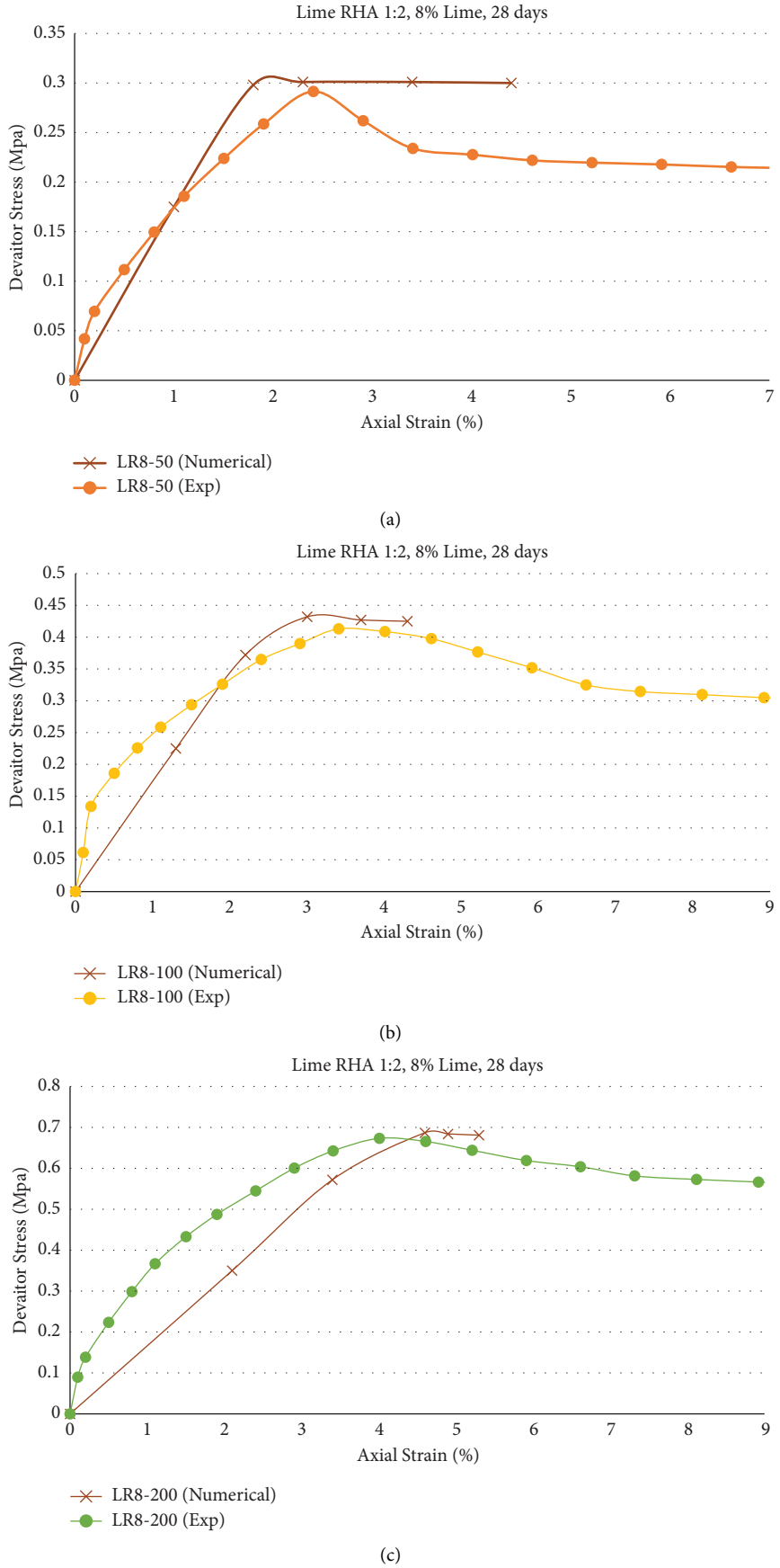

Figure 11: Deviator stress-strain curves for 8% LRHA treated soil (1 : 2) after 28 days of curing, under three different confining pressures of (a) 50, (b)100, and (c) 200 kPa.

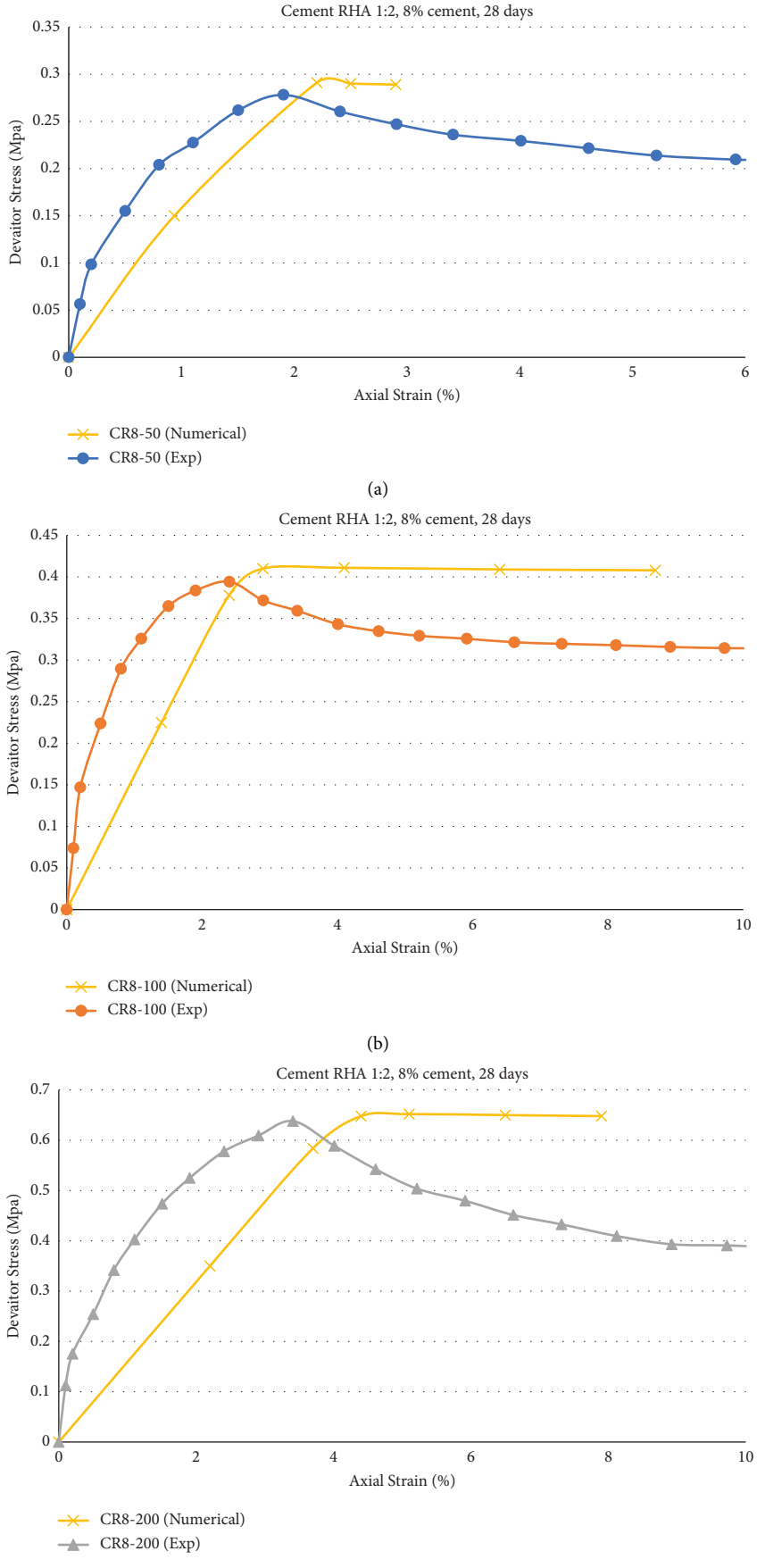

Figure 12: Deviator stress-strain curves for 8% CRHA treated soil (1 : 2) after 28 days of curing, under three different confining pressures of (a) 50, (b)100, and (c) 200 kPa.

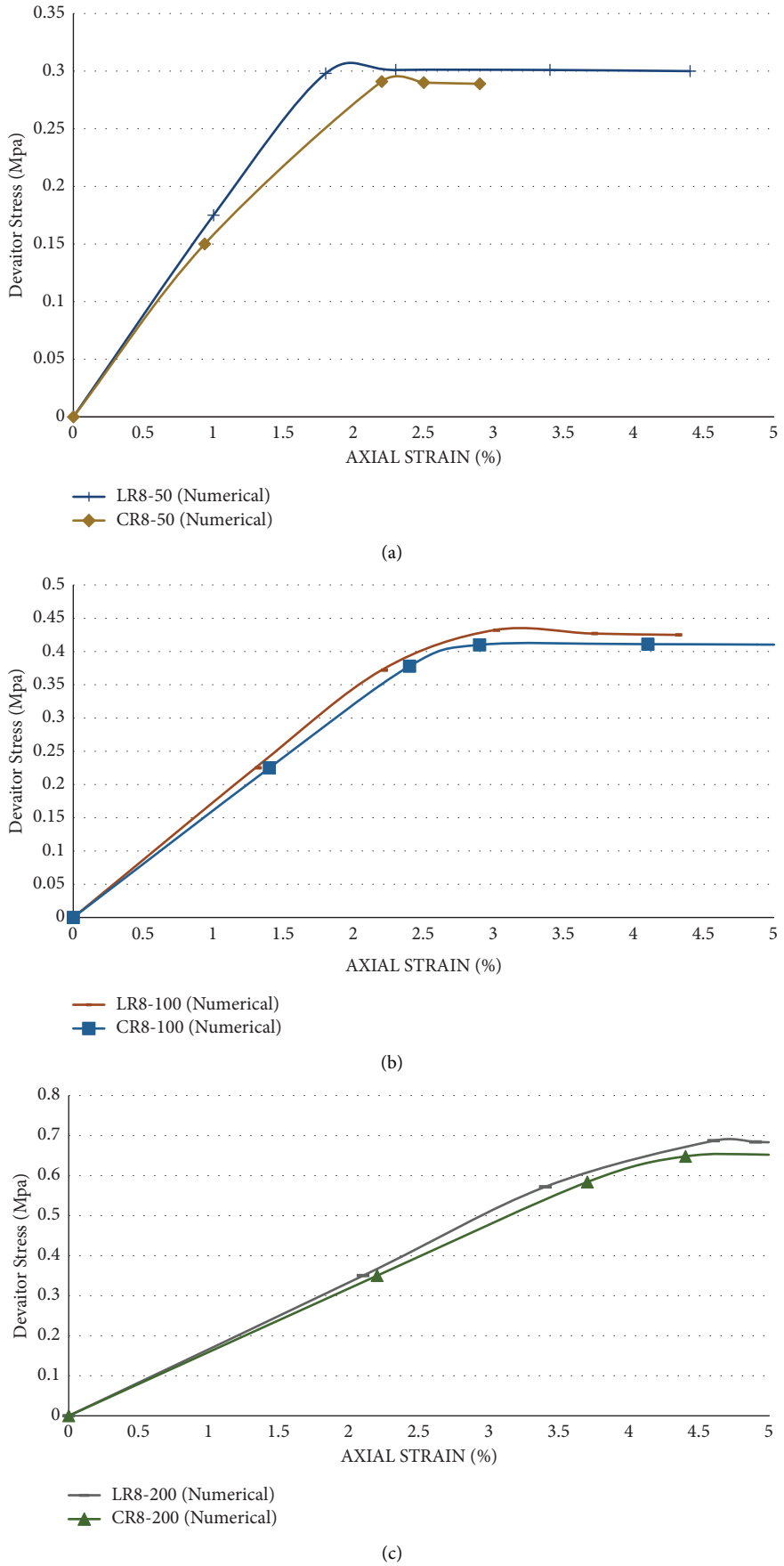

Figure 13: Comparison between deviator stress-strain curves for 8% CRHA and 8% LRHA treated soil (1 : 2) after 28 days of curing, under three different confining pressures of (a) 50, (b)100, and (c) 200 kPa.

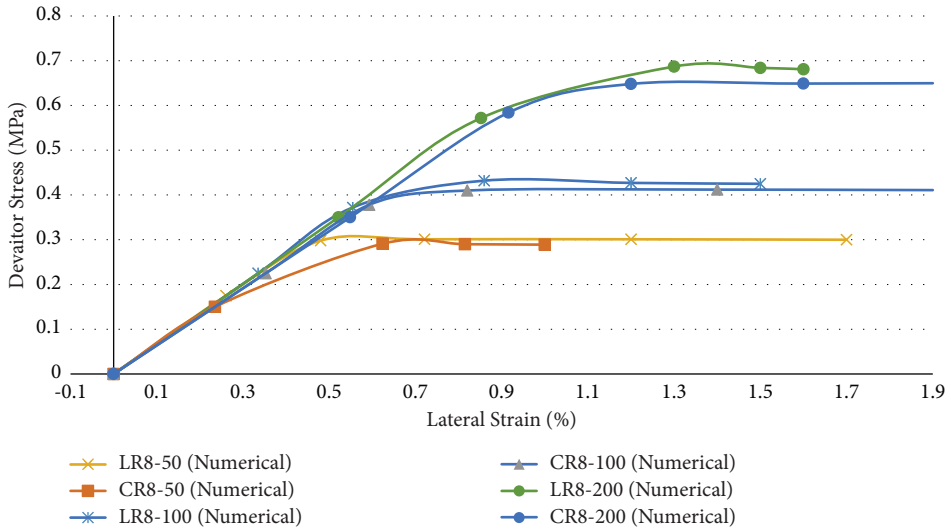

Figure 14: Comparison between deviator stress-lateral strain curves for 8% CRHA and 8% CRHA treated soil (1 : 2) after 28 days of curing.

of 100 kPa and 200 kPa. The calculated deviator stresses for LR8-50, LR8-100, and LR8-200 tests compared with CR8-50, CR8-100, and CR8-200 tests, increased by 3%, 5%, and 5%, respectively.

The graph of lateral strains each shows a minimal difference between LR8 and CR8 for each confining stress (Figure 14). Overall, as the confining stresses increase, the calculated lateral stains gradually increase in the middle of the model. The calculated deviator stresses are very close to each other at similar confining stresses in all parts of the curves. The graph demonstrates that the stress in all LR8 models is higher than in CR8 models. This shows the effect of the LRHA mixture in stabilizing the soft soil and that the performance of LRHA-treated samples under vertical load is better than samples treated with cement.

The deviator stresses at failure obtained by the FE method and experimental results are listed in Table 5. As can be seen, the numerical modelling results are very similar to the experimental results.

Overall, the comparison between numerical modelling and the triaxial test demonstrates that the numerical modelling results agree well with the test results. This implies that the Mohr–Coulomb model's implementation in the finite element program is performed correctly to calculate the final stage of failure results.

4.3. Shear Strength Determination. Figures 15 and 16 show Mohr–Coulomb circles plotted by RocData (3.013) based on the major stresses calculated from PLAXIS. RocData is used based on the triaxial or direct shear strength data. Software calculates the parameters of the linear and nonlinear strength envelopes and Mohr–Coulomb [19]. As shown in Figure 15, the calculated cohesion and friction angles of the specimens in PLAXIS are in good agreement with the experimental results (see Table 6).

Table 5: Comparison of experimental and FEM results at failure.

Test	Method	Deviator stress (kPa)*10^{-3}	Axial strain (%)
LR8-50	Experimental	291	2.4
	FEM	301	2.3
LR-100	Experimental	413	3.4
	FEM	432	3.0
LR-200	Experimental	673	4.0
	FEM	687	4.6
CR8-50	Experimental	278	1.9
	FEM	291	2.2
CR8-100	Experimental	394	2.4
	FEM	411	4.1
CR8-200	Experimental	638	3.4
	FEM	652	5.1

5. Result

It is established that the FE analysis is a suitable technique for determining the influence of lime and cement on the strength parameters. As the experimental result, the numerical modelling also showed that the cement and lime had almost similar strength behaviour.

The results from the triaxial test and numerical modelling are presented in Figure 17. This figure demonstrates the evolution of axial strain with the deviator stress, which has been plotted to show the strong correlation with the stress-strain curves obtained from the compression test. The triaxial test panels are based on the three tests (LR8-50, 100, and 200). The peaks detected in experimental analysis and the numerical calculations demonstrate approximately similar values, and the results showed an accurate match in comparing the triaxial tests performed in the laboratory.

As it is shown in Figure 17, the axial strain increased with an increase in the strain. In all these three tests (ID 1, 2, and

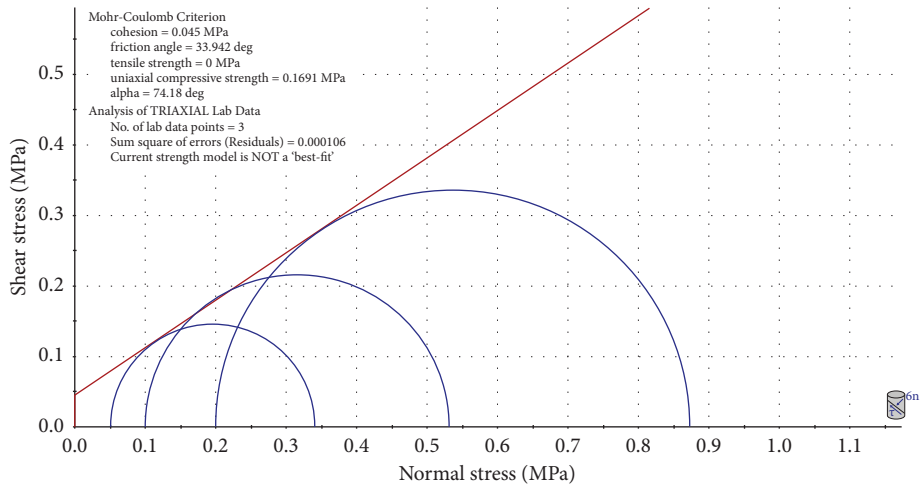

Figure 15: Shear strength variation against the normal stress-saturated condition LR8 (lime RHA 1 : 2 and 8% lime content), 28 days of curing, from numerical modelling plotted by RocData.

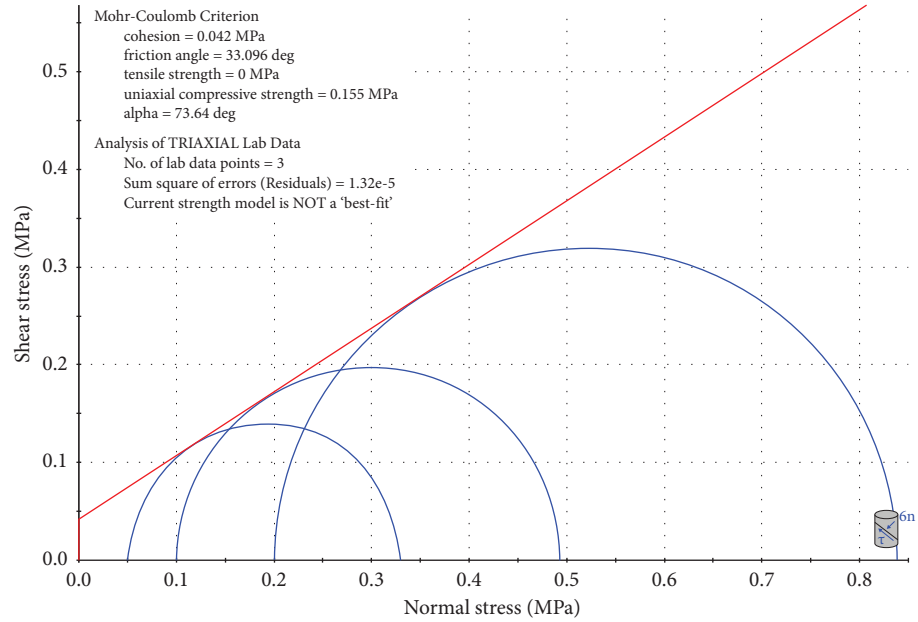

Figure 16: Shear strength variation against the normal stress-saturated condition CR8 (cement RHA 1 : 2 and 8% lime content), 28 days of curing, from numerical modelling plotted by RocData.

Table 6: Comparison between cohesion and internal friction angle obtained from the triaxial test and numerical simulation.

Triaxial test			Numerical test		
Sample	Cohesion (kPa)	Internal friction (ϕ)	Sample	Cohesion (kPa)	Internal friction (ϕ)
LRHA – 1 : 2 (8%)	46	34	LRHA – 1 : 2 (8%)	45	33.94
CRHA – 1 : 2 (8%)	46	33	CRHA – 1 : 2 (8%)	42	33.09

3), in the beginning, the rates of increase in the axial strain were almost similar, but in the ID 1 test, the rates remained unchanged after the deviatoric stress exceeded 300 kPa. On the contrary, in the ID 2 test, after the deviatoric stress exceeded 350 kPa, the axial strain started to increase dramatically from 20 to 50 kPa at 430 kPa. It is clear that, for the last test ID 3, the axial strain continued to change until 35 kPa, after which it rose again, but more significantly to 72 in 680 kPa.

It is also observed that the axial strain at failure increases with an increase in confining stress. Changes to the geometry configuration cause a significant out-of-balance force. The finite element mesh is under a series of forces using the load advancement ultimate level procedure. The staged process is

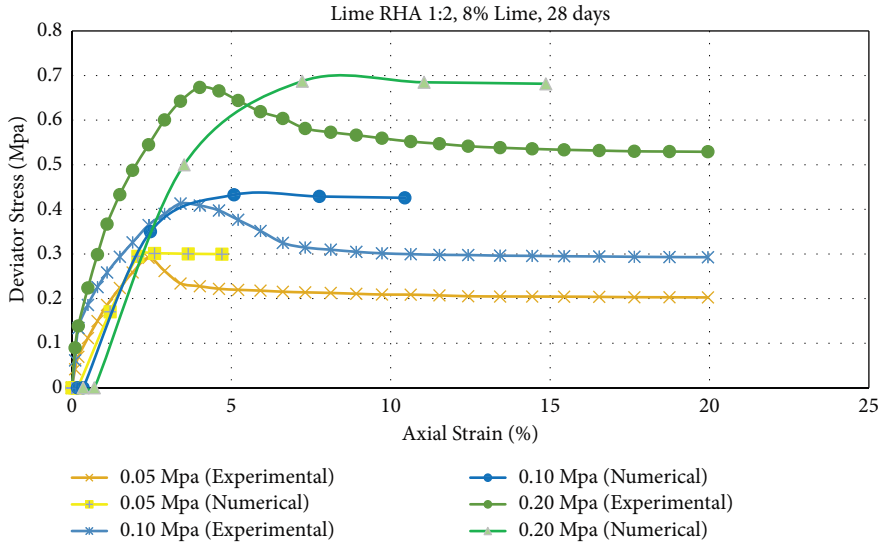

Figure 17: Correlation/validation of treated soil behaviour under triaxial compression. Stress deviation vs. axial strain (numerical and experimental)-LRHA treated soil.

controlled by a multiplier that is increased from zero to the ultimate level (Σ_M stage). In each stage, when the Σ_M stage reaches 1, it means that the model has reached an ultimate load; at that moment, the calculation stops, and no more data will be released as a result by the software. This is the reason that the numerical curves do not show the strain-softening section.

6. Conclusion

A laboratory experimental study has been carried out on treated soil samples under triaxial loading conditions, and finite element simulation has been carried out using the PLAXIS 2D computer program. The main part of this study was investigating and comparing the results from axisymmetric modelling and a solution in terms of vertical settlement and stress in soil samples. The applicability of the result was also examined by the verification of parametric analyses for use in practical work.

The following conclusions can be drawn based on findings from this research:

(1) comparison between CRHA and LRHA samples in terms of displacement, axial strain, and deviatoric stress demonstrates that LRHA is a suitable alternative to a CRHA mixture since the strength and deformation parameters show a great result compared to similar research. The triaxial test result and PLAXIS simulation both confirm that the treated soil with LRHA considers a good replacement for the CRHA mixture in terms of strengthening the soft soil.

(2) The variation in deviatoric stress and volume change against axial strain in a single-stage triaxial test was plotted, and the maximum deviatoric stress appeared to increase significantly from the samples mixed with lime to the samples treated with cement as the effective stress increased from 50 to 200 kPa.

(3) It has been observed that the peak deviator stress values of treated soil with LRHA increase with the increase in density of the stabilizers.

(4) The FE analysis results for peak deviator stress values found reasonably good agreement with the experimental results. The variation was in the range of 1.22%–4.10%.

(5) Comparison between the axial strain and deviatoric stress curves from numerical tests demonstrates good correlations with similar patterns compared to the triaxial test result.

(6) The result of the 2D unit cell encased column model showed good agreement in general with those from the analytical solution, vertical displacement, stress, and strain on LRHA soil samples. The results given by the numerical analyses are more in agreement with the analytical solution if the confining pressure chosen is 200 kPa. On the contrary, analyses for validation showed a numerical simulation of soil treated with CRHA in PLAXIS.

Data Availability

The datasets generated and analyzed during the current study can be obtained from the corresponding author upon reasonable request.

Conflicts of Interest

The authors declare that they have no conflicts of interest.

Acknowledgments

Bentley/Seequent has funded this publication.

References

[1] S. P. Leatherman, "Shoreline stabilization approaches in response to sea level rise: U.S. experience and implications for Pacific Island and Asian nations," *Water, Air, and Soil Pollution*, vol. 92, no. 1–2, pp. 149–157, 1996.

[2] V. Boumboulis, D. Apostolopoulos, and N. Depountis, "The importance of geotechnical evaluation and shoreline evolution in coastal vulnerability index calculations," *Mar. Sci. Eng. Artic.*vol. 9, 2021.

[3] D. Mujah, M. E. Rahman, and N. H. M. Zain, "Performance evaluation of the soft soil reinforced ground palm oil fuel ash layer composite," *Journal of Cleaner Production*, vol. 95, pp. 89–100, May 2015.

[4] M. S. Imbabi, C. Carrigan, and S. McKenna, "Trends and developments in green cement and concrete technology," *International Journal of Sustainable Built Environment*, vol. 1, no. 2, pp. 194–216, 2012.

[5] P. Rodrigues, J. D. Silvestre, I. Flores-Colen et al., "Evaluation of the ecotoxicological potential of fly ash and recycled concrete aggregates use in concrete," *Applied Sciences*, vol. 10, no. 1, p. 351, 2020.

[6] A. G. L. Lees and J. Clausen, "Strength envelope of granular soil stabilized by multi-axial geogrid in large triaxial tests," *Canadian Geotechnical Journal*, vol. 57, no. 3, pp. 448–452, 2020.

[7] X. Yang, Y. Zhang, and Z. Li, "Embankment displacement plaxis simulation and microstructural behavior of treated-coal gangue," *Minerals*, vol. 10, no. 3, p. 218, 2020.

[8] M. Kahlström, "Plaxis 2D comparison of mohr-coulomb and soft soil material," *Delft Univ. Technol. PLAXIS bv Netherlands*, 2011.

[9] L. S. Wong and S. Somanathan, "Analytical and numerical modelling of one-dimensional consolidation of stabilized peat," *Civil Engineering J.*vol. 5, no. 2, p. 398, 2019.

[10] R. Brinkgreve, W. M. Swolfs, E. Engin et al., *Plaxis 2d Reference Manual Connect*, Plaxis bv, Netherlands, 2011.

[11] F. Kasim, A. Marto, B. A. Othman, I. Bakar, and M. F. Othman, "Simulation of safe height embankment on soft ground using plaxis," *APCBEE Procedia*, vol. 5, pp. 152–156, 2013.

[12] S. Kalla, "*Modeling studies to assess long term settlement of lightweight aggregate embankment*," M.S. thesis, University of Texasat Arlington, Arlington, TX, USA, 2010.

[13] N. Dirgėlienė, A. Norkus, J. Amšiejus, Š. Skuodis, and D. Žilioniene, "Stress-strain analysis of sand subjected to triaxial loading," *The Baltic Journal of Road and Bridge Engineering*, vol. 8, no. 1, pp. 25–31, 2013.

[14] K. Harichane, M. Ghrici, and S. Kenai, "Effect of curing time on shear strength of cohesive soils stabilized with combination of lime and natural pozzolana," *International Journal of Civil Engineering*, vol. 9, no. 2, pp. 90–96, 2011.

[15] X. Jiang, Z. Huang, F. Ma, and X. Luo, "Analysis of strength development and soil-water characteristics of rice husk ash-lime stabilized soft soil," *Materials*, vol. 12, pp. 3873–3923, 2019.

[16] Z. Song, D. Zhang, Y. Mao, Y. Mu, K. Zhang, and Q. Zhang, "Behavior of lime-stabilized red bed soil after cyclic wetting-drying in triaxial tests and SEM analysis," *Advances in Materials Science and Engineering*, vol. 2020, Article ID 4230519, 12 pages, 2020.

[17] Y. H. Wang and S. C. Leung, "Characterization of cemented sand by experimental and numerical investigations," *Journal of Geotechnical and Geoenvironmental Engineering*, vol. 134, no. 7, pp. 992–1004, 2008.

[18] B. Ukritchon, J. C. Faustino, and S. Keawsawasvong, "Numerical investigations of pile load distribution in pile group foundation subjected to vertical load and large moment," *Geomech. Eng.*vol. 10, no. 5, pp. 577–598, 2016.

[19] F. Zahri, M. L. Boukelloul, R. Hadji, and K. Talhi, "Slope stability analysis in open pit mines of Jebel Gustar Career, Ne Algieria- a multi-steps approach," *Mining Science*, vol. 23, pp. 137–146, 2016.